

NASA/TM—2011-210987



# Active-Controlled Fluid Film Based on Wave-Bearing Technology

*Florin Dimofte*  
*University of Toledo, Toledo, Ohio*

*Robert C. Hendricks*  
*Glenn Research Center, Cleveland, Ohio*

## NASA STI Program . . . in Profile

Since its founding, NASA has been dedicated to the advancement of aeronautics and space science. The NASA Scientific and Technical Information (STI) program plays a key part in helping NASA maintain this important role.

The NASA STI Program operates under the auspices of the Agency Chief Information Officer. It collects, organizes, provides for archiving, and disseminates NASA's STI. The NASA STI program provides access to the NASA Aeronautics and Space Database and its public interface, the NASA Technical Reports Server, thus providing one of the largest collections of aeronautical and space science STI in the world. Results are published in both non-NASA channels and by NASA in the NASA STI Report Series, which includes the following report types:

- **TECHNICAL PUBLICATION.** Reports of completed research or a major significant phase of research that present the results of NASA programs and include extensive data or theoretical analysis. Includes compilations of significant scientific and technical data and information deemed to be of continuing reference value. NASA counterpart of peer-reviewed formal professional papers but has less stringent limitations on manuscript length and extent of graphic presentations.
- **TECHNICAL MEMORANDUM.** Scientific and technical findings that are preliminary or of specialized interest, e.g., quick release reports, working papers, and bibliographies that contain minimal annotation. Does not contain extensive analysis.
- **CONTRACTOR REPORT.** Scientific and technical findings by NASA-sponsored contractors and grantees.

- **CONFERENCE PUBLICATION.** Collected papers from scientific and technical conferences, symposia, seminars, or other meetings sponsored or cosponsored by NASA.
- **SPECIAL PUBLICATION.** Scientific, technical, or historical information from NASA programs, projects, and missions, often concerned with subjects having substantial public interest.
- **TECHNICAL TRANSLATION.** English-language translations of foreign scientific and technical material pertinent to NASA's mission.

Specialized services also include creating custom thesauri, building customized databases, organizing and publishing research results.

For more information about the NASA STI program, see the following:

- Access the NASA STI program home page at <http://www.sti.nasa.gov>
- E-mail your question via the Internet to [help@sti.nasa.gov](mailto:help@sti.nasa.gov)
- Fax your question to the NASA STI Help Desk at 443-757-5803
- Telephone the NASA STI Help Desk at 443-757-5802
- Write to:  
NASA Center for AeroSpace Information (CASI)  
7115 Standard Drive  
Hanover, MD 21076-1320

NASA/TM—2011-210987



# Active-Controlled Fluid Film Based on Wave-Bearing Technology

*Florin Dimofte*  
*University of Toledo, Toledo, Ohio*

*Robert C. Hendricks*  
*Glenn Research Center, Cleveland, Ohio*

Prepared for the  
International Symposium on Stability Control of Rotating Machinery (ISCORMA 2001)  
sponsored by the Bently Rotor Dynamics Research Corporation  
South Lake Tahoe, California, August 20–24, 2001

National Aeronautics and  
Space Administration

Glenn Research Center  
Cleveland, Ohio 44135

*Level of Review:* This material has been technically reviewed by technical management.

Available from

NASA Center for Aerospace Information  
7115 Standard Drive  
Hanover, MD 21076-1320

National Technical Information Service  
5301 Shawnee Road  
Alexandria, VA 22312

Available electronically at <http://www.sti.nasa.gov>

# Active-Controlled Fluid Film Based on Wave-Bearing Technology

Florin Dimofte  
University of Toledo  
Toledo, Ohio 43606

Robert C. Hendricks  
National Aeronautics and Space Administration  
Glenn Research Center  
Cleveland, Ohio 44135

## Summary

It has been known since 1967 that the steady-state and dynamic performance, including the stability of a wave bearing, are highly dependent on the wave amplitude. A wave-bearing profile can be readily obtained by elastically distorting the stationary bearing sleeve surface. The force that distorts the elastic sleeve surface could be an applied force or pressure. The magnitude and response of the distorting force would be defined by the relation between the bearing surface stiffness and the bearing pressure, or load, in a feedback loop controller. Using such devices as piezoelectric or other electromechanical elements, one could step control or fully control the bearing. The selection between these systems depends on the manner in which the distortion forces are applied, the running speed, and the reaction time of the feedback loop. With these techniques, both liquid- (oil-) or gas- (air-) lubricated wave bearings could be controlled. This report gives some examples of the dependency of the bearing's performance on the wave amplitude. The analysis also was proven experimentally.

## Introduction

Classic bearings, such as lemon, lobe, tilt pad, and concentric Rayleigh Step bearings are noted in Zaretsky's book on bearings (1997) as well as in his "Life Factors for Rolling Bearings" (1992) in conjunction with the time-dependent loading of a piston engine. Several papers related to stability in lemon, tilt pad, and lobe bearings were also considered in the Bently symposium, ISCORMA 2001 (Bently, 2001). Although these bearings are of great importance, in this paper we will concentrate on wave bearings. First we will look into methods to control rotordynamic vibrations, then walk through wave-bearing analysis, and finally, corroborate with experimental data.

Vekteris (1993) proposed a method for classifying several types of bearings, including autoadaptive and adaptively controllable fluid-film bearings with either continuous or intermittent feedback adjustments. Without causing conflict between the two methods, one may state that, for a given bearing application, two ways to enhance stability are to (1) control bearing pressure and (2) control geometry. The means of control may be passive or active with fixed-point adjustment or a feedback loop.

One of the early means of pressure control was given by Girard (1851, as referenced in Stout et al., 1978), who used a hydrostatic bearing at the Paris Industrial Exposition in 1878 (Girard (1863, as referenced in Stout et al., 1978). Oil was pumped down four legs of a table that supported a large mass, into hydrostatic pads with sufficient pressure to support the mass. The table could be moved about with ease. Lord Rayleigh (1917, as referenced in Stout et al., 1978) used two ground pennies to control the geometry, and with tap water as the lubricant, illustrated the principles of the fluid-film thrust bearing. (Rayleigh added his "two cents" worth. Perhaps Emile Nouguier and Maurice Koechlin, employed by Eiffel, used the Girard concept in the tower (June 1884).)

## Geometry

These devices rely on distortion of the bearing geometry to adjust the fluid-film thickness, which alters bearing load capacity. The devices may act directly on the bearing, or as dampers, or both. Active devices add complexity and weight to the system and have potential failure modes of their own; yet in some cases, using these devices is the only way to achieve stability.

Schuller (1967, 1973) introduced a three-lobed (wave) bearing with a plain journal  $R$  and isolated-shims between the bearing and bearing housing. For more details, see Appendix A. The shims distorted the bearing harmonically in the form of a sine wave about a mean bearing radius ( $R_{PC}$  = pitch circle); bearing wave amplitudes  $H_L$  ranged from 0.025 mm in steps of nearly 0.025 to 0.102 mm; others included 0.015 and 0.066 mm. Schuller reported that, without axial grooves, it was nearly impossible to maintain stability for minimum clearances  $C$  above 0.018 mm, where  $C = R_{PC} - R$ , and that the lobes lost their effectiveness for  $C > 0.013$  mm. The highest stability was found for the 0.025-mm bearing amplitude with axial grooving, implying that there is an optimum lobe amplitude. For bearings without axial grooving, a similar trend was noted. Lund (1968) analyzed the lobe bearing yet considerably overpredicted the onset of instability (by a factor of 3 or more).

The reported stability data trends for the Schuller wave bearing *without* axial grooves follow from Appendix A for  $0.025 \text{ mm} \leq H_L \leq 0.076 \text{ mm}$ :

$$\langle M \rangle \Gamma^2 = [18M/(P_a L)] (C/R) \omega^2 \sim 100$$

For three-lobe bearings *with* axial grooves, the mean stability locus for data with  $H_L < 0.066$  is  $\langle M \rangle \Gamma \sim 1$ , and for all data presented,  $\langle M \rangle \Gamma \sim 1/3$ , where (symbols are also defined in Appendix B)

$$\langle M \rangle = M P_a (C/R)^5 / (2\mu^2 L) \text{ and } \Gamma = 6\mu\omega (R/C)^2 / P_a$$

$\langle M \rangle$  mass parameter

$M$  mass carried by the bearing

$\Gamma$  bearing speed parameter

$P_a$  ambient pressure

$L$  bearing length

$\omega$  rotational speed

$\mu$  viscosity

This implies that, for a given geometry and working fluid, the instability threshold is strongly dependent on the rotation speed; yet surprisingly, it is inversely proportional to the ambient pressure.

Dimofte (1995a) initiated an improvement in forming the wave amplitude by using mechanical screws in the bearing housing to distort the bearing with additional analysis for dynamics (for wave bearing design and dynamic analysis (also see Dimofte et al. (2011)). Experimental work on a three-wave journal bearing was reported in Dimofte and Hendricks (1996). A two-wave bearing with a stiffness orthotropy ( $K_{xx} \gg K_{yy}$ ) was also tested (Dimofte and Hendricks, 1995). In these experiments, a strong dependence of the bearing stability on the wave amplitude was found.

Palazzolo et al. (1988) cited the extensive literature covering active control of bearings and proposed the use of piezoelectric pushers as active vibration control devices in test components at the NASA Lewis Research Center (now NASA Glenn), Figure 1. The usual application is to provide minute position adjustments of lenses and mirrors in laser systems. The ceramic stacked discs are connected in parallel electrically and expand in response to applied voltage. The extension depends on the number and



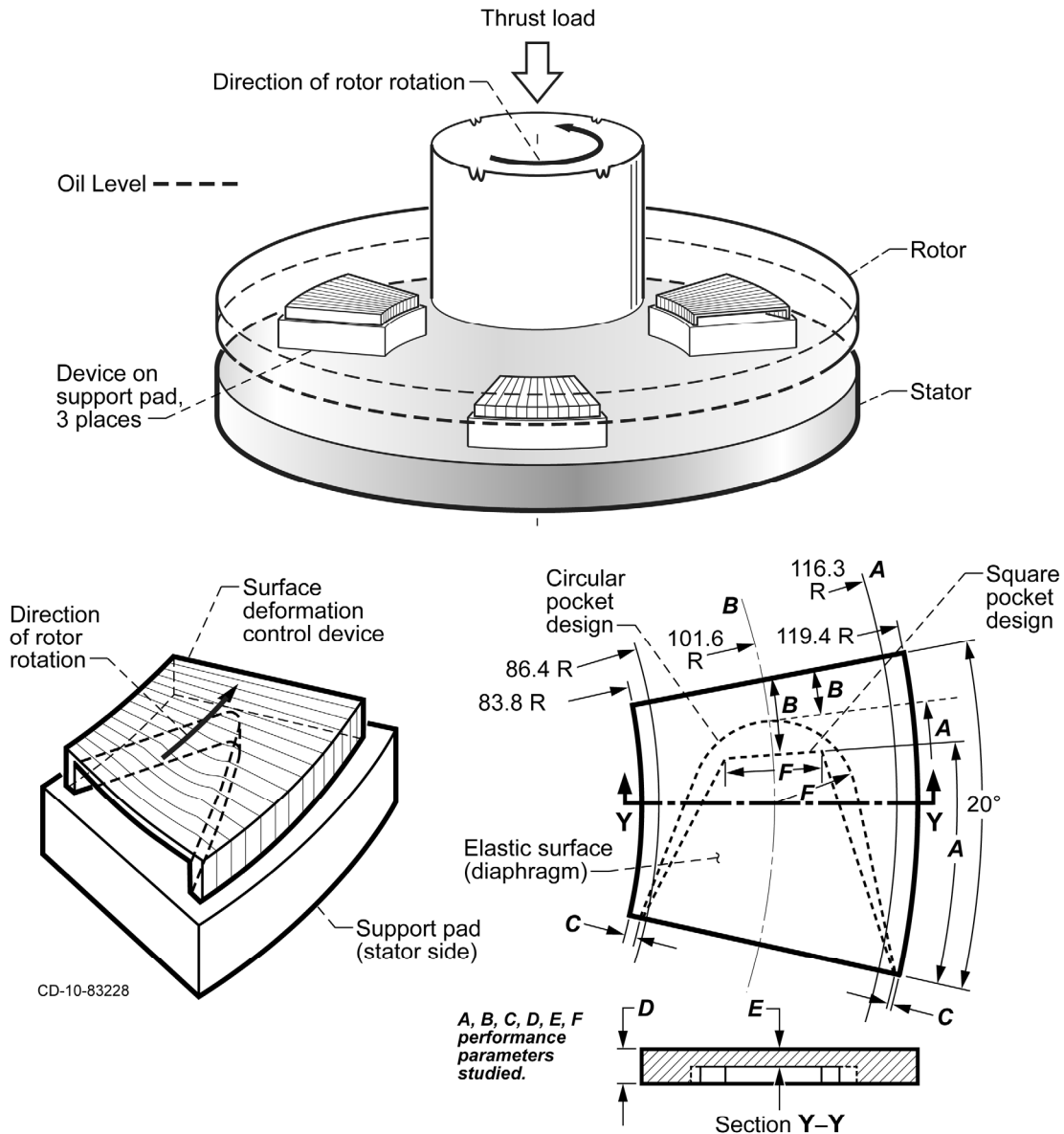


Figure 2.—Surface deformation control device—thrust plate diaphragm deformation with step and shroud fully flooded lubrication (derived from information in Hemingway, 1967, and Kettleborough, 1957, as referenced in Hemingway, 1967). Total area of three pads, 37.8 cm<sup>2</sup>. All dimensions are in millimeters.

## Pressure

These devices rely on restrictors, pockets, or the motion of intermediate surfaces to stabilize and enhance bearing load capacity. In all cases, special attention must be given to the restrictor design relative to the moving surface and pocket because poorly designed restrictors can destabilize the bearing. Most devices function better at decreased eccentricities with small changes in control volume flows. (See the pioneering work on flows in pocket/restrictor visualization and computation by Braun and Dzodzo, 1997.)

Constantinescu et al. (1971) extended the work of Mayer and Shaw (1963) and the work proposed by de Gast (as referenced in Bassani and Piccigallo, 1992), Figure 3. In this system, a double-acting pressure regulator supplied pressures to orthogonally opposed pairs of hydrostatic pockets on the  $X$ - $Y$  axis to



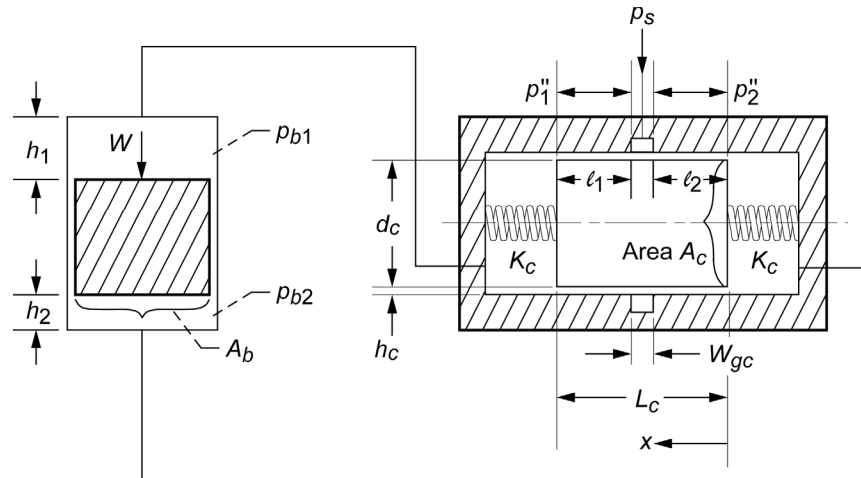


Figure 3.—Differential pressure control device (Mayer and Shaw, 1963).  
 $p_s = \text{constant}$ .  $W$ , weight;  $p_{b1}$  and  $p_{b2}$ , pressures at piston positions  $b1$  and  $b2$ ;  $h_c$ , clearance;  $K_c$ , equivalent spring stiffness. Copyright ASME; used with permission.

control the journal position. The balanced diaphragms admitted pressure to the hydrostatic pockets as the journal moved off axis toward the pocket and drained pressure from the opposing pocket, thereby providing a restoring force on the journal. Simplicity characterizes this device, yet its response is limited to hydromechanical response time. Line and regulator size along with control fluid characteristics are factors in the design.

Yoshimoto and Kikuchi (1999) described a self-controlled restrictor with control features similar to that of Constantinescu et al. (1971). Their floating disc responded to journal motions through a series of capillaries and an oil source, which function as a damper to provide a differential force across the disc; in turn, this force was transmitted through the pocket to the journal. Another pressure balance device, which used a fixed diaphragm to form both the pocket and the fluid displacement to control the journal, was studied by Rowe et al. (1974). The device performed well with water, but it had some pneumatic instabilities when operated with air.

Lewis (1984) examined the effect of capillary, orifice, and flow-control valve compensation in hydrostatic cylindrical-pad bearings and cautioned that stiffness may approach zero with a fixed-aperture orifice or a capillary, but that it does not occur with flow-control valves. Aperture size determines when instabilities will arise.

Sato et al. (1988) used an actively controlled orifice with the appropriate phase lag to control the air film thickness and achieved enhanced stiffness and damping. Details on the compensation circuit are vague.

Hongo et al. (1987) used piezoelectric constriction of a cylinder (capillary) to control a thrust bearing. The measured film thickness and bearing load capacity signals were fed through an analog-to-digital converter, and bearing stiffness and radial response position were computed. In turn, the differential between the measured and desired settings was translated into an electrical impulse that slaved the piezoelectric constrictors, completing the feedback loop. Hongo et al. found that (1) the bearing stiffness could be greatly enhanced over certain ranges in fluctuating loads and (2) the film thickness could be held constant within the submicron range.

Yoshimoto et al. (1994) balanced the fluid forces acting on each side of a floating disc to control the airflow entering the thrust bearing clearance, and they proposed an optimum design method. Their reported stiffnesses are an order of magnitude greater than for conventional thrust bearings. Later, Yoshimoto and Kamiyama (1995) used a floating brush seal as a self-controlled restrictor, balancing the pressures acting on the brush to control gas flows into the bearing entrance. They proposed an optimum high-stiffness design. Yoshimoto and Kamiyama (1995) also extended the floating brush concept to

control journal bearings, again balancing the pressure differentials to control gas flow into the bearing. Again, the optimization method was discussed and found useful in enhancing bearing stiffness.

Blondeel and Snoeys (1974) used a membrane over a V-gutter sandwiched between the bearing housing and the bearing. The membrane was sealed by O-rings with differential control restrictors, as in squeeze films, to provide local distortion of the bearing. These changes enhanced load capacity, resulted in high bearing stiffness, and reduced gas consumption and clogging.

San Andres (1992) analyzed a journal bearing perturbed about its centered position to show that with end seals, the bearing has enhanced stability and damping as well as lower flow rates. San Andres extended the analogies to squeeze film dampers, yet cautioned that if excessively tight end seals are used, the bearing's direct stiffness can be lost (no flow, no support).

Bently (2000) described a fully lubricated, pressurized (nominally <7 MPa) ServoFluid Control Bearing as one that enhances load capacity and stability. The four pocket/land combinations and restrictors isolated and mitigated fluid rotation, providing lower average circumferential fluid-film speed/journal speed [ $\lambda$ ] and eccentricities  $\epsilon$  as well as a near-zero attitude angle. In their discussion (p. 296) in Mayer and Shaw (1963), Fox et al. suggested using an axial drain groove midway between adjacent pockets to make the bearing less sensitive to circumferential flows. The enhanced pocket/restrictor pressure permitted an axial versus circumferential support pressure wedge (similar to a center-balanced seal experiment with John Vance's flow blocks). Consequently, the bearing operated at lower eccentricities ( $\epsilon \sim 0.05$  to  $0.25$ ) and tighter overall clearances, and the lower  $\lambda$  mitigated negative fluid-engendered stiffness and damping. The W-shaped bearing stiffness and U-shaped damping with radial position provided high restoring forces at high eccentricities, more notably for liquid lubricants. The external controls of the restrictors were not discussed.

In a five-part paper, Stout et al. (1978) offered general design guidelines, material selections, geometry, and system designs for fluid-film bearings. Abduljabbar et al. (1996) described a closed-loop control system that used bearing position and unbalance forces as input parameters to the controller to enhance rotor-bearing system performance.

Rozeanu and Snarsky (1978) suggested that every time the boundary layer is disturbed, the hydrodynamic behavior of the bearing is improved.

Morishita and Ura (1993) proposed the use of electrorheological (ER) fluid, vibration control actuators, and an adaptive neural-network control system suitable for the control of ER actuators in a shock absorber system for automobiles, a squeeze film damper bearing for rotational machines, a dynamic damper for multi-degree-of-freedom structures, and a vibration isolator. The modes of a simple beam were shown to be reduced. Feng and Xin (1987) demonstrated computer-assisted control of shaft vibrations.

## **Magnetic Lubricant/Seal**

Yoshida et al. (1996) described a 2.5-in. hard disk drive supported by a magnetic-fluid-film bearing. The spindle unit stator was 20 mm with a 0.3-mm shaft. The drive reduced nonrepeatable runout to less than 0.05  $\mu\text{m}$ . Each lobe of the bearing was asymmetrical. The unit consisted of a motor, a bearing, and a hub. The bearing and motor were both inside the hub, and the shaft was fixed to the hub. A magnetic fluid was used as both lubricant and sealant. The bearing had three lobes at  $120^\circ$ , with similar nominal displacements, to form minimum clearances at the trailing edge with a gap between each lobe for maintaining lubricant supply. The thrust bearings had tapered land structures at  $120^\circ$  and a groove at the leading edge for lubricant supply. Test data at stiffnesses of 1 and 5 kN/mm show a three-fold increase in runout with a temperature increase from 5 to 55  $^\circ\text{C}$ .

## Wave-Bearing Concept as a Tool to Control Bearing and Bearing-Rotor Performances

The wave-bearing concept could be placed in the geometry category of surface deformation. Unlike the plain journal bearing (Fig. 4(a)), a wave journal bearing (Dimofte, 1995b; Schuller, 1967, 1973) is a bearing with a slight, but precise, variation in its circular profile such that a waved profile is circumscribed on the inner bearing diameter and the wave amplitude is equal to a fraction of the bearing clearance. Figure 4(b) shows a three-wave bearing. The clearance, the wave, and the wave's amplitude are greatly exaggerated in Figures 4(a) and (b) so that the concept can be visualized.

A three-wave bearing geometry can be obtained by applying three forces on the bearing sleeve. These forces will deform the sleeve from the circular shape. If the forces are varied, various wave amplitudes can be obtained (Fig. 5). The wave-bearing performance strongly depends on the wave amplitude. Since 1993, it has been found that both the bearing stability related to the subsynchronous whirl motion (SSWM) generated by the fluid film and the bearing dynamic coefficients can be modified by changing the wave amplitude. Schuller (1967, 1973) arrived at similar experimental results (see Appendix A).

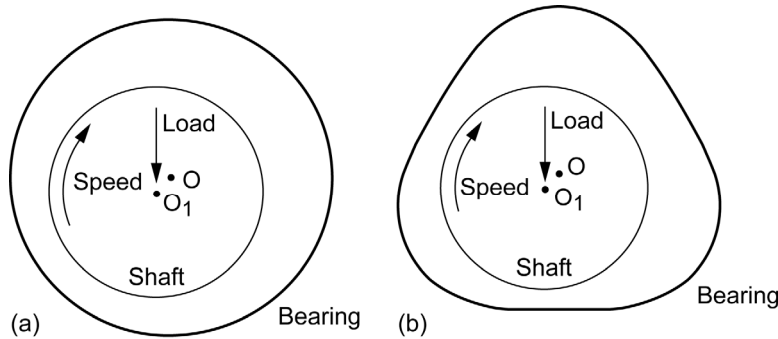


Figure 4.—Journal bearings. (a) True circular. (b) Three-wave.

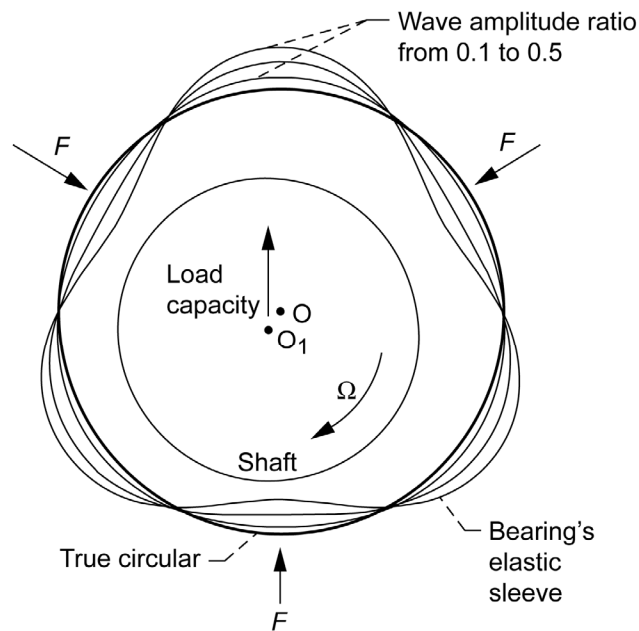


Figure 5.—Wave bearing with various wave amplitudes.

The capacity of the wave bearing to reduce the journal bearing sensitivity to SSWM was demonstrated theoretically in Dimofte (1995b). A parametric study over a broad range of bearing parameters indicated that the wave journal bearing offers better stability than the plain journal bearing under all operating conditions. However, the wave journal bearing's performance depends on the wave amplitude and increases significantly as the wave amplitude increases (within limits) (also see Appendix A).

In addition, experimental work on gas wave journal bearings proved the numerical prediction (Dimofte and Hendricks, 1996). Dimofte and Hendricks also found that an unloaded journal bearing with an altered circular profile, such as a wave bearing, allows operation over a range of speeds under which the bearing can run free of SSWM, whereas the plane journal bearing is unstable. When the wave journal bearing starts developing SSWM, the radius of this motion increases to a size where the equilibrium between the radial force generated by the whirl movement and the pressure force in the film is established. The equilibrium radius is smaller than the bearing clearance, and the bearing can run stably and safely.

The strong dependence of the wave-bearing steady-state and dynamic performance on the wave amplitude can be used to control bearing behavior by changing the wave amplitude. That has been mentioned since 1967 on the basis of wave-bearing analysis (Dimofte, 1993; Schuller, 1967, 1973). In addition, the possibility of controlling the bearing's dynamics by actively controlling the bearing surface profile was also reported (Rylander et al., 1995). In that case, an elliptic bearing shape (close to a two-wave bearing) was used. Rylander et al. found that active bearing deflection control can significantly reduce vibration in a machine. Also, Dimofte and Hendricks (1995) reported the strong stabilizing effect in the case of a two-wave bearing that shows a stiffness orthotropy.

New strong arguments about the major effect of the wave amplitude on bearing performance are reported herein on the basis of bearing performance calculations that are compared with experimental results reported by Dimofte et al. (1996). Bearing dynamic characteristics were calculated according to the method outlined in Dimofte (1995b). Thus, experiments were conducted and calculations were performed on a gas journal bearing with a 50-mm diameter, a 58-mm length, and a 0.016-mm radial clearance. These measurements were taken when the bearing was inspected at 21 °C. Both bearing stability and bearing dynamic coefficients were investigated to support the active control concept on the basis of a wave-bearing configuration.

## Bearing Stability

The unloaded condition was selected because of the maximum sensitivity of the gas journal bearings to the SSWM under such a condition. Numerical calculations were performed over a broad range of bearing parameters. Thus, speeds up to 30 000 rpm, wave amplitude ratios (wave amplitude divided by radial clearance, WAR) from 0 to 0.6, and radial clearances from 10 to 25  $\mu\text{m}$  were used in the calculation. The results are plotted in Figure 6. The circular bearing (WAR = 0.0) was found to be unstable at any speed, unlike wave bearings, which can operate stably at any speed less than a threshold that depends on the WAR and the radial clearance. If the bearing reaches this speed threshold, it switches from a stable to an unstable operating condition. This speed threshold increases as both the WAR and the clearance increase. The WAR has the most significant effect on this speed threshold at larger clearances rather than at small clearances.

Experimental results from Dimofte et al. (1996) and Dimofte and Keith (1998) are also plotted in Figure 6. Various WAR's (0.024, 0.157, 0.187, 0.22, 0.28, and 0.3) were obtained by applying various sets of forces  $F$  (Fig. 5). The bearing profile was inspected each time that the forces were modified. Figure 7 shows four of these profiles. The bearing stability was observed on the wave journal bearing tester at NASA Glenn, and the experimental procedure is well explained in the report (Dimofte et al., 1996). Bearing temperatures were recorded during all experiments. The bearing running temperature ranged from 15 °C when the first test was performed to 35 °C for the last test because of the difference in time

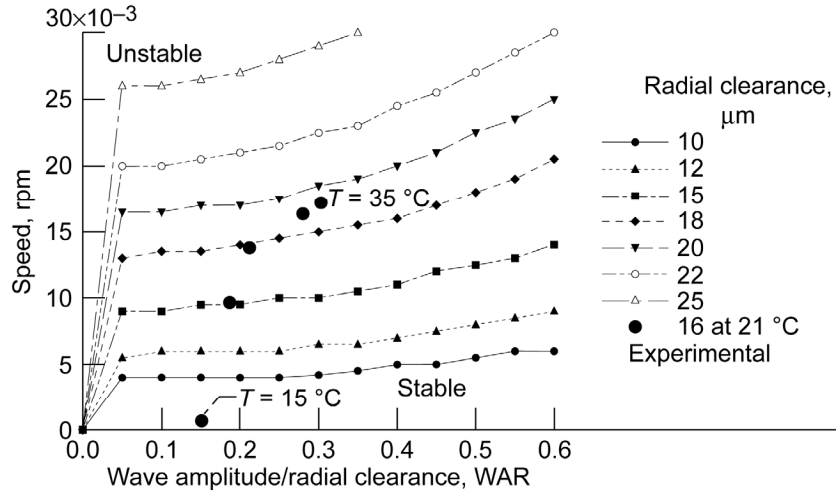


Figure 6.—Predicted stability curves—threshold speed versus WAR—of an unloaded three-wave gas journal bearing. Diameter,  $D$ , 50 mm; length,  $L$ , 58 mm. Test results are plotted for five cases.

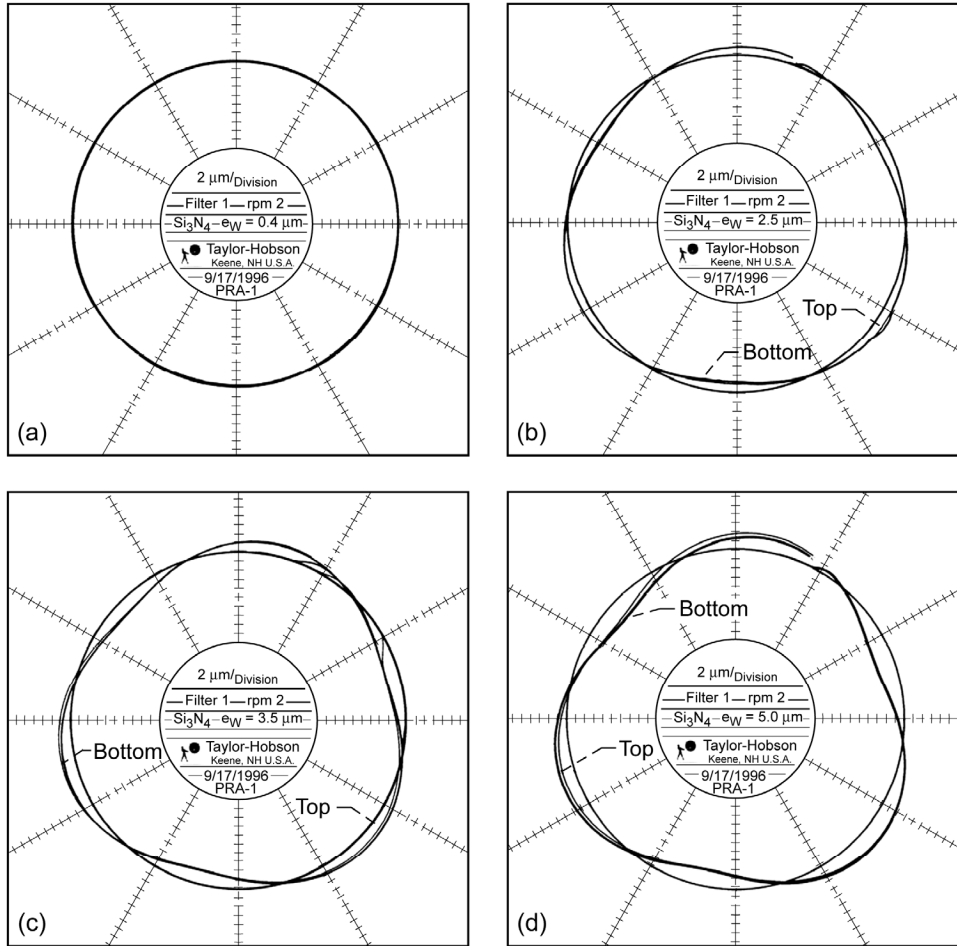


Figure 7.—Test bearing profiles;  $e_W$ , wave amplitude. (a) True circular; wave amplitude/radial clearance, WAR, 0.024. (b) WAR, 0.157. (c) WAR, 0.22. (d) WAR, 0.30.

and speed between tests when SSWM was observed. Therefore, the actual bearing clearance when the bearing operated at each test varied from the inspected clearance (at 21 °C) in a range of a few micrometers.

### Bearing Dynamic Coefficients

The numerical results of bearing performance show that the WAR has a strong influence on the bearing direct stiffness coefficient  $K_{xx}$  (Fig. 8). The WAR effect increases as speed increases, and a WAR of 0.5 can double the circular bearing stiffness if the bearing running speed is over 15 000 rpm. The other bearing dynamic coefficients are less influenced by the WAR. Therefore, plots for the direct damping coefficient (Fig. 9) could be typical for all bearing coefficients except the direct stiffness.

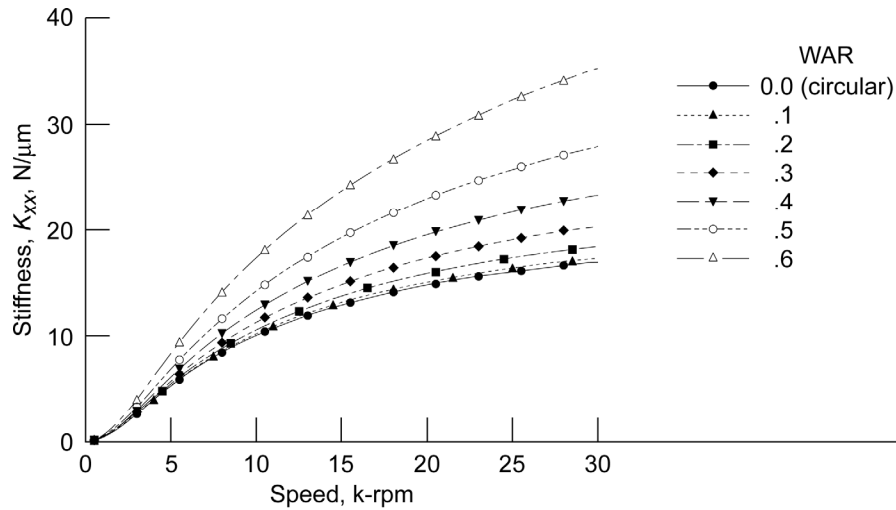


Figure 8.—Predicted direct stiffness versus speed at various wave amplitude/radial clearances (WARs) of an unloaded three-wave gas journal bearing. Diameter,  $D$ , 50 mm; length,  $L$ , 58 mm.

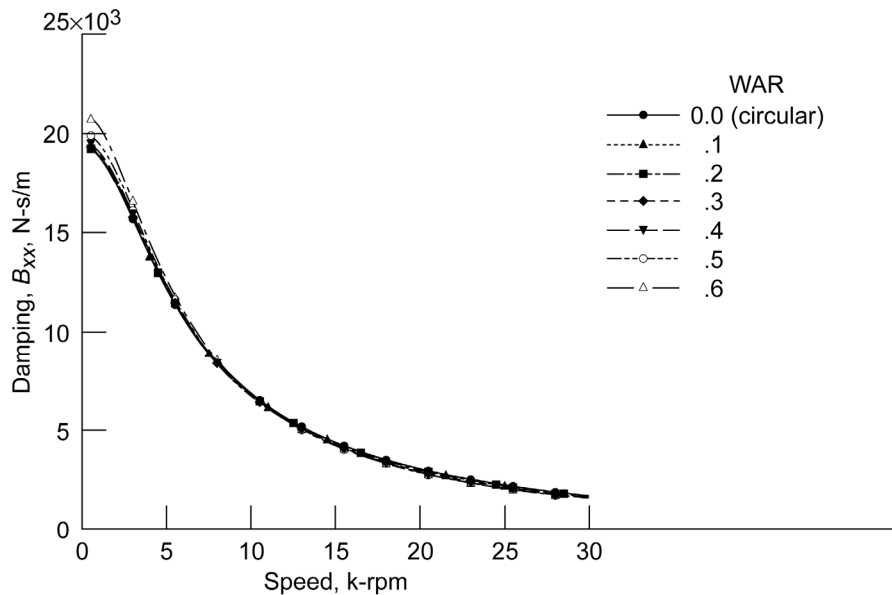


Figure 9.—Predicted direct damping versus speed at various wave amplitude/radial clearances (WARs) of an unloaded three-wave gas journal bearing. Diameter,  $D$ , 50 mm; length,  $L$ , 58 mm.

## Conclusions

Changes in pressure or geometry are ways to activate a fluid-film bearing that have been investigated for a good period of time. In the geometry category, and based on the experimental and analytical work herein, the wave-bearing concept could be efficiently used to develop an active fluid-film bearing. Bearing wave amplitude can be modified by the controlling system (1) to alter the load capacity while keeping the bearing stable and (2) to modify the bearing's dynamic coefficients to control the rotordynamic behavior.

The bearing (wave) profile can be easily modified by applying external forces; devices such as piezoelectrics, stepper motors, and hydraulics with feedback controls and programmed analysis can be used. These forces must have a short response time; the actual value of this time depends on the bearing running speed.





## Appendix A.—Schuller’s Three-Lobe Bearing Experiments

In Schuller’s experiments (1967, 1973), the vertical assembled bearing inside diameter (ID) was nominally 38 mm (1.5 in.) with a length-to-diameter ratio (L/D) of unity (Fig. 10).

The inside surfaces (ID) of the three-lobe bearings (Fig. 11) and the outside surfaces (OD) of the journals were machined to a root-mean-square finish of 0.1 to 0.2  $\mu\text{m}$  (4 to 8  $\mu\text{-in.}$ ). The journals were either stainless steel or Stellite material, and the bearing was of bronze. The runout of the journal on the test shaft averaged 5  $\mu\text{m}$  (200  $\mu\text{-in.}$ ).

It is important to realize the differences between a three-lobed journal and a three-lobed bearing. The convergent-divergent *lobed journal* is as in Figure 11(a), the convergent-divergent *lobed bearing* is as in Figure 11(b) and a *three-lobed wave bearing* is as in Figure 12 and is the type used in this report.

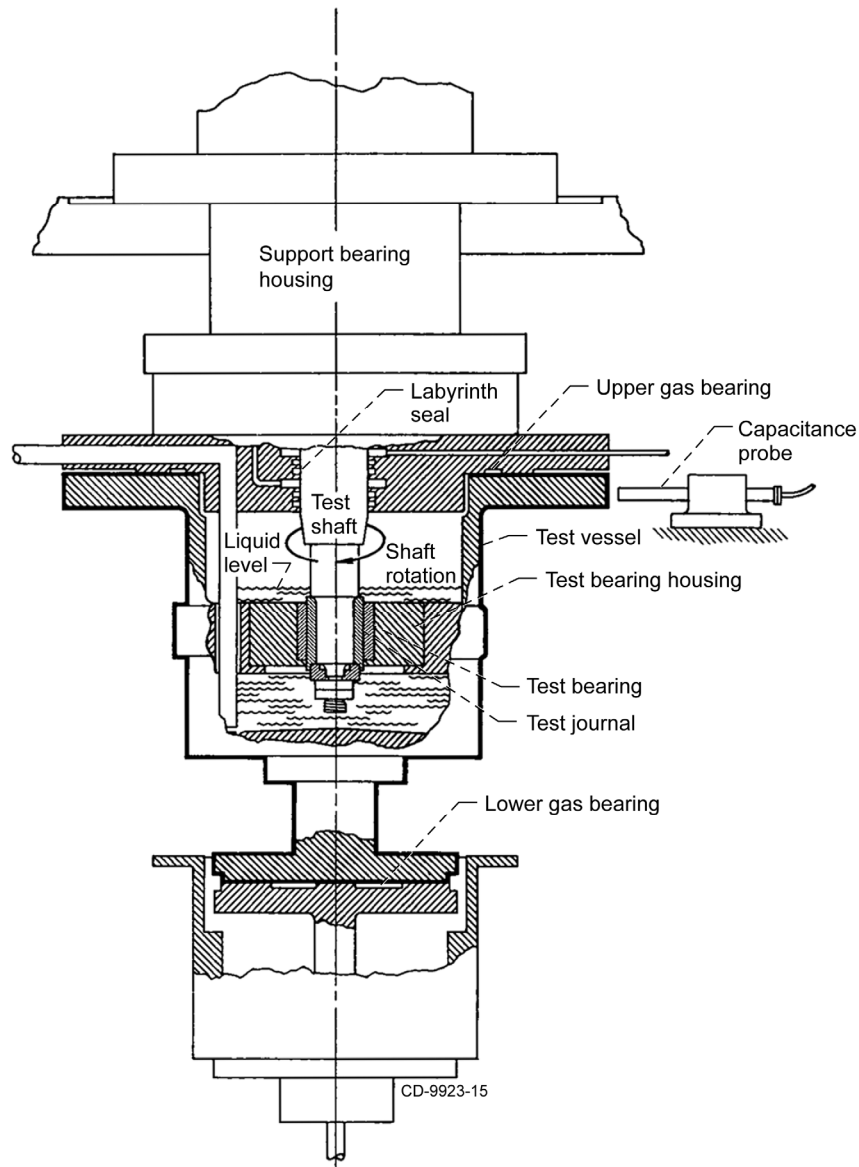


Figure 10.—Schuller’s bearing test apparatus. From Figure 10, Schuller (1973).

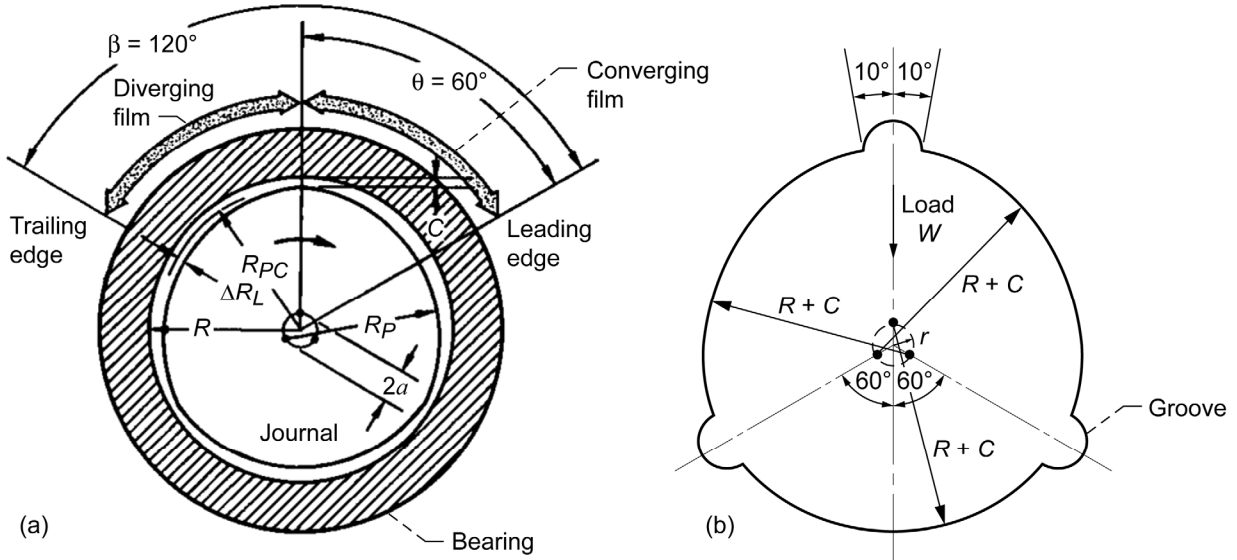


Figure 11.—Convergent-divergent three-lobed journal and bearing.  $C$ , bearing radial clearance;  $R$ , bearing radius. (a) Centrally lobed (converging-diverging) configuration for three-lobe journal geometry.  $\beta$ , sector arc length;  $\theta$ , arc length from leading edge of sector to line along which the lobe is preloaded radially;  $\Delta R_L$ , leading-edge entrance wedge thickness;  $R_{PC}$ , radius of pitch circle;  $R_P$ , lobe radius;  $a$ , preload (ellipticity). From Figure 5(b), Schuller (1973). (b) Classic three-lobe bearing.  $R$ , journal radius;  $C$ , radial clearance; preload  $\delta = r/C$ , where  $r$  is the eccentric position of radius  $R + C$ . From Figure 1, Lund (1968).

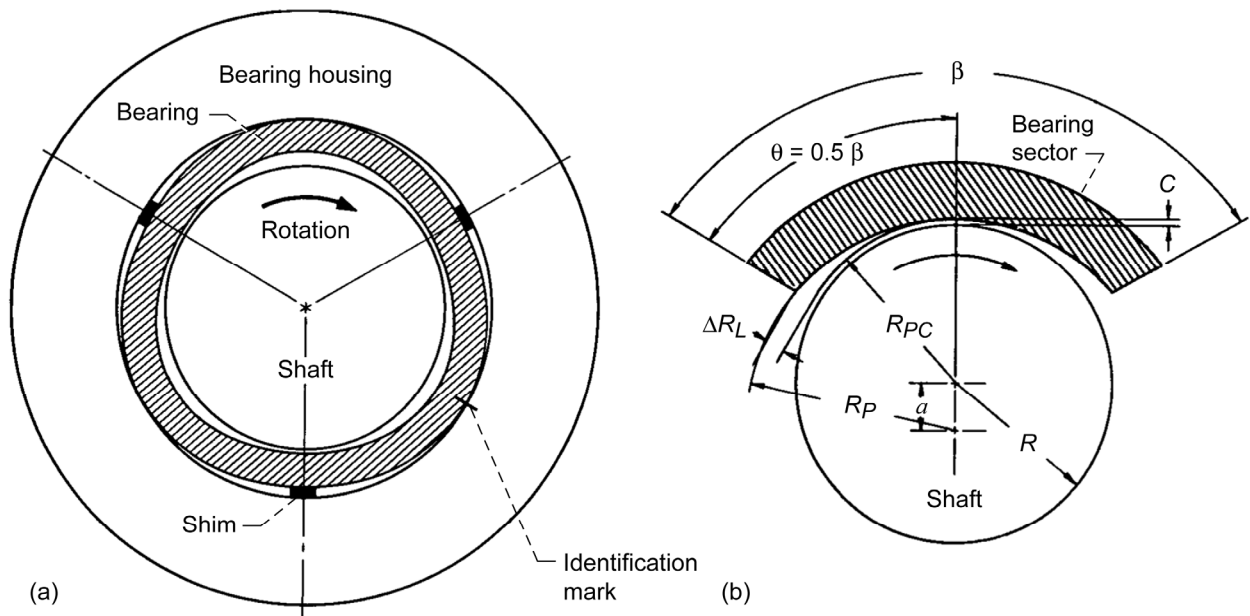


Figure 12.—Three-lobe sinusoidal (wave) bearing fabrication methodology. (a) Bearing assembly. (b) Bearing geometry. Offset factor  $\alpha = 0.5$ , where  $\alpha = \theta/\beta$ , the arc length from the leading edge of a sector to the line along which the lobe is preloaded radially, divided by the arc sector length.  $C$ , bearing radial clearance;  $R$ , bearing radius.  $\Delta R_L$ , leading-edge entrance wedge thickness;  $R_{PC}$ , radius of pitch circle;  $R_P$ , lobe radius. From Figures 3(a) and (b), Schuller (1973).

Of the many innovative features of Schuller's work, we cite here only one, that of fabricating the lobes.

Lobe heights  $H_L$  were determined by shims placed between the bronze bearing and the stainless steel housing. For example, three 0.025-mm (1000- $\mu$ -in.) equally spaced shims placed around and between the bronze bearing OD and the stainless housing provide three lobes with that same height. The bronze bearing ID was 38.149 mm (1.5039 in.) (Fig. 12). The shimmed bearing interfaces provided a sinusoidal-wave/fluid-film interface (Schuller, 1967, 1973).

Schuller tested 10 three-central-lobe bearings with and without three axial grooves (Fig. 13(a) and (b), respectively). The bearings had different lobe heights (wave amplitudes), journal diameters, and clearances. The radial clearance  $C$  ranged from 0.009 to 0.052 mm (350 to 2050  $\mu$ -in.), and  $H_L$  ranged from 0 to 0.102 mm (0 to 4000  $\mu$ -in.).

Schuller used journals with different diameters to obtain the clearances shown for any particular bearing tested (Fig. 13). A total of 39 bearing stability tests were conducted at  $C$  ranging from 0.009 to 0.052 mm (350 to 2050  $\mu$ -in.) and  $H_L$  ranging from 0 to 0.102 mm (0 to 4000  $\mu$ -in.).

Figure 13(a) shows the stability limits of a three-lobe, three-axial-groove bearing at five lobe heights. Increasing  $H_L$  from 0 to 0.025 mm (0 to 1000  $\mu$ -in.), increased the stability, but increasing  $H_L$  from 0.025 to 0.066 mm (1000 to 2600  $\mu$ -in.) decreased the stability. For the limited bearing set tested, the maximum stability occurred at an  $H_L$  (wave amplitude) of 0.025 mm (1000  $\mu$ -in.).

It is interesting to note the range of stability of the three-central-lobe bearing with and without axial grooves. It was impossible to attain stable operation at  $C > 0.018$  mm (700  $\mu$ -in) with the three-central-lobe bearing without the three axial grooves.

For three-lobe bearings *with* axial grooves, the mean stability locus for data with  $H_L < 0.066$  was  $\langle M \rangle \Gamma \sim 1$ , and for all data,  $\langle M \rangle \Gamma \sim 1/3$ .

For three-lobe bearings *without* axial grooves, as in the case of our work described in the text, the mean stability locus for data with  $H_L < 0.066$  was  $\langle M \rangle \Gamma^2 \sim 100$  (Fig. 13(b)) and for data with  $H_L > 0.066$  was  $\langle M \rangle \Gamma \sim 1/3$ , which is more closely aligned to stability data limits for the axially grooved bearings (Fig. 13(a)).

It is also noted that an unloaded plain journal bearing (zero wave amplitude) will whirl at all speeds and clearances; however small loads or misalignments can provide a preload resulting in a limited degree of stability.

Dimofte et al. have continued to refine and improve wave bearing design and analysis contributing to diverse applications such as turbomachine and turbine engine applications. For the interested reader, these recent efforts are documented in a book chapter (Dimofte et al., 2011)

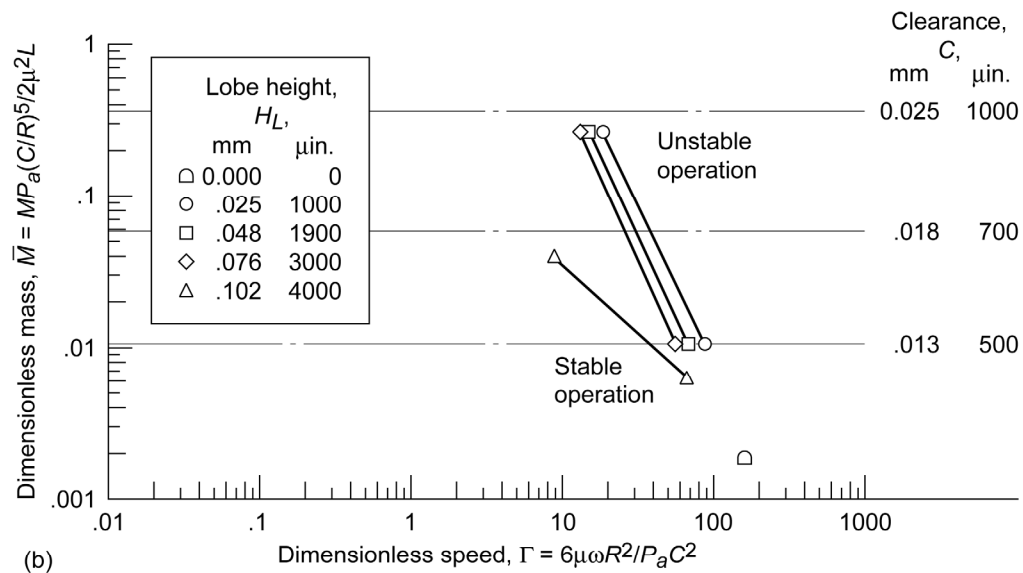
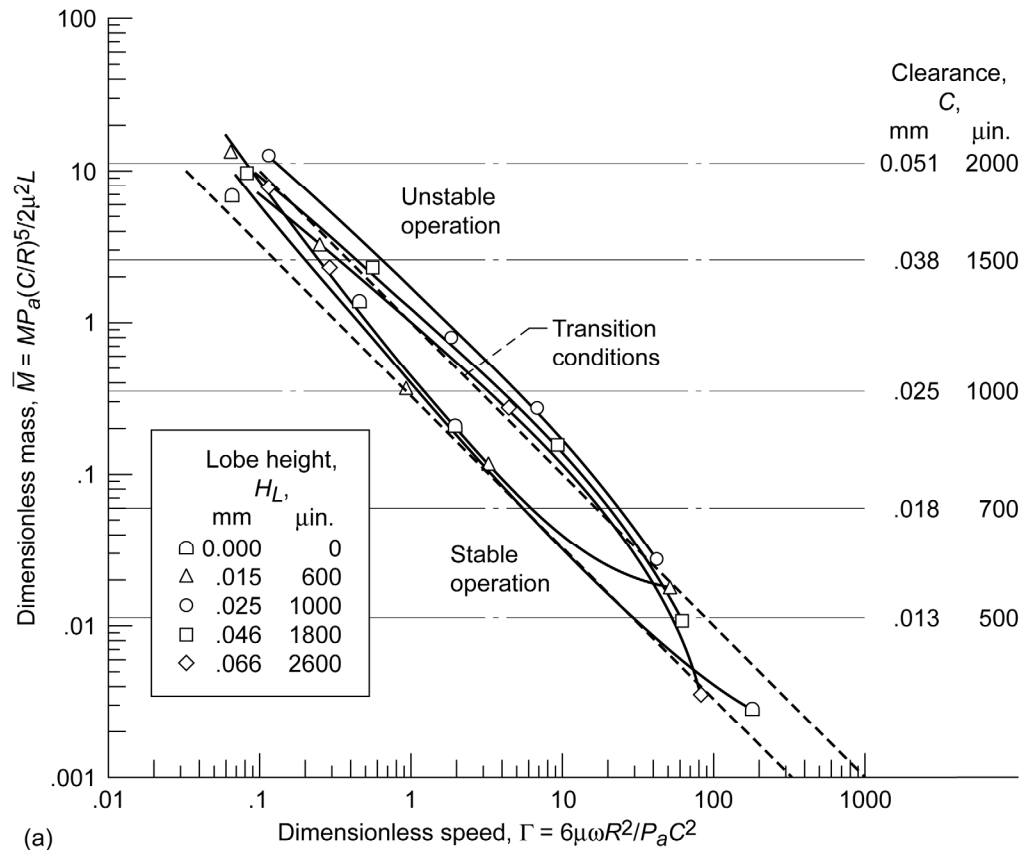


Figure 13.—Effect of lobe height  $H_L$  on the stability of a three-central-lobe bearing. (a) With three axial grooves. (b) Without grooves.  $C$ , bearing radial clearance;  $\bar{M}$ , dimensionless mass parameter;  $M$ , rotor mass per bearing;  $P_a$ , atmospheric pressure;  $R$ , journal or bearing radius;  $\mu$ , lubricant dynamic viscosity;  $L$ , bearing length;  $\Gamma$ , dimensionless speed parameter;  $\omega$ , journal angular speed. From Figure 31, Schuller (1973).

## Appendix B.—Symbols

$A$	area
$a$	preload (ellipticity), mm (in.)
$C$	bearing radial clearance, mm (in.)
$C_O$	bearing radial clearance at zero preload, $(R_P - R)$ , mm (in.)
$D$	journal diameter, cm (in.)
$d_c$	diameter of displacement cylinder, cm (in.)
$d_1, d_2, d_3, d_4$	displacement position (1, 2, 3, or 4), cm (in.)
$dt$	derivative with respect to time, sec
$e_w$	wave amplitude
$F$	force
$G$	amplifier gain
$g$	gravitational constant, W/g m/sec <sup>2</sup> , (in./sec <sup>2</sup> )
$H_L$	lobe height, cm (in.)
$h$	height
$h_c$	clearance, cm (in.)
ID	inside diameter or surface
$K_A$	pusher driver stiffness, N/m (lb/in.)
$K_c$	equivalent spring stiffness, N/m (lb/in.)
$K_{xx}$	stiffness coefficient
$K_\phi$	angular stiffness, N/m (lb/in.)
$L$	bearing length, cm (in.)
$M$	rotor mass per bearing, W/g, kg (lb-sec <sup>2</sup> /in.)
$\langle M \rangle$	or $\bar{M}$ , dimensionless mass parameter, $M P_a (C/R)^5 / 2\mu^2 L$
$me$	eccentric test mass, g (lb)
OD	outside diameter or surface
$P_a$	atmospheric pressure, N/m (psia)
$p_{b1}, p_{b2}$	pressure at piston position $b_1$ or $b_2$ , N/m (psia)
$R$	journal or bearing radius, cm (in.)
$\Delta R_L$	leading-edge entrance wedge thickness, mm (in.)
$R_P$	lobe radius, cm (in.)
$R_{PC}$	radius of pitch circle, cm (in.)
$r$	eccentric position of radius $(R + C)$ , where $R$ is the bearing radius and $C$ is the clearance

$S_A$	piezoelectric vertical pusher drive potential, V/m
$S_D$	piezoelectric horizontal pusher drive potential, V/m
$W$	weight, N (lb)
$\alpha$	offset factor, $\theta/\beta$
$\beta$	sector arc length, deg
$\Gamma$	dimensionless speed parameter, $6\mu\omega (R/C)^2/P_a$
$\delta$	preload ( $r/C$ )
$\lambda$	average circumferential fluid-film speed/journal speed
$\varepsilon$	bearing eccentricity
$\theta$	arc length from leading edge of sector to line along which lobe is preloaded radially, deg
$\mu$	lubricant dynamic viscosity, N-sec/m (lb-sec/in.)
$\omega$	journal angular speed, rad/sec
SSWM	subsynchronous whirl motion
WAR	wave amplitude divided by radial clearance

## References

- Abduljabbar, Z.; ElMadany, M.M.; and AlAbdulwahab, A.A. (1996): Active Vibration Control of a Flexible Rotor. *Comput. Struct.*, vol. 58, no. 3, pp. 499–511.
- Bassani, Roberto; and Piccigallo, Bruno (1992): *Hydrostatic Lubrication: Theory and Practice*. Elsevier.
- (De Gast, J.G.C. (1967): A New Type of Controlled Restrictor (M.D.R) for Double Film Hydrostatic Bearings and Its Applications to High-Precision Machine Tools. *Adv. in Machine Tools Design and Research, Proceedings of the 7th International MTDR Conference, Birmingham*, pp. 273–298. Pergamon Press, Oxford, New York.)
- Bently, Donald E. (2000): In Pursuit of Better Bearings, *ORBIT*, Second Quarter 2000, vol. 21, no. 2, pp. 33–42. <http://www.bpb-co.com/articles/00pursuit.php>
- Bently, Donald E. (2001): *ISCORMA-1, The 1st International Symposium on Stability Control of Rotating Machinery*. South Lake Tahoe, CA.
- Blondeel, E.; and Snoeys, R. (1974): Externally Pressurised Bearing With Pressure Dependent Restrictors. Paper D2, *Proceedings of the 6th International Gas Bearing Symposium*, N.G. Coles, ed., BHRA Fluid Engineering, Cranfield, U.K., pp. D2–19 to D2–41.
- Braun, M.J.; and Dzodzo, M.B. (1997): Three-Dimensional Flow and Pressure Patterns in a Hydrostatic Journal Bearing Pocket. *J. Tribology*, vol. 119, pp. 711–719.
- Constantinescu, V.N., et al. (1971): On the Possibilities of Improving the Operating Characteristics of Externally-Pressurised Gas Films. Presented at the 5th Gas Bearing Symposium, Southampton, England.
- Dabrowski, Leszek; Olszewski, Olgierd; and Wasilczuk, Michal (1998): New Generation of Hydrodynamic Thrust Bearing. Paper presented at the 1998 STLE Annual Meeting, Detroit, MI.
- Dimofte, F.A. (1993): Waved Journal Bearing Concept—Evaluating Steady-State and Dynamic Performance With a Potential Active Control Alternative. *Vibration of Rotating Systems*, K.W. Wang and Dan Segalman, eds., Presented at the 1993 ASME Design Technical Conference, 14th Biennial Conference on Mechanical Vibration and Noise. ASME, New York, NY, pp. 121–128.
- Dimofte, Florin (1995a): Predicted and Experimentally Observed Fluid Film Instability of an Unloaded Gas Journal Bearing. Paper presented at the 15th Canadian Congress of Applied Mechanics—CANCAM 95, University of Victoria, Victoria, BC, pp. 978–979.
- Dimofte, F. (1995b): Wave Journal Bearing With Compressible Lubricant—Part I: The Wave Bearing Concept and a Comparison With a Plain Circular Bearing. *Tribol. Trans.*, vol. 38, no. 1, pp. 153–160.
- Dimofte, Florin; and Hendricks, Robert C. (1995): Two- and Three-Wave Journal Bearing Fractional Whirl Motion, *Proceedings of SES'95: Society of Engineering Science 32nd Annual Technical Meeting*, Society of Engineering Science, New Orleans, LA, pp. 773–774.
- Dimofte, Florin; and Hendricks, Robert C. (1996): Fractional Whirl Motion in Wave Journal Bearings. *Seals Code Development Workshop*, NASA CP-10181, pp. 337–340. <http://ntrs.nasa.gov/>
- Dimofte, Florin; Keith, Theo G., Jr.; and Hendricks, Robert C. (1997): Gas Journal Bearing Stability Versus Amplitude Ratio. *Seals/Secondary Flows Workshop 1996*, Vol. 2, NASA CP-10198 (Final Technical Report for Experimental Evaluation of Journal Bearing Stability and New Gas Wave Bearing Materials. NASA Grant NCC3-553, 1998, Robert C. Hendricks, ed., pp. 855–864.
- Dimofte, F.; and Keith, T.G, Jr. (1998): Wave Bearing Technology to Control Journal Bearing Dynamics. *Proceedings of the Seventh International Symposium on Transport Phenomena and Dynamics of Rotating Machinery, ISROMAC-7*, Feb. 22–26, Honolulu, HI, vol. 1, pp. 327–336.
- Dimofte, Florin; Ene, Nicoleta M.; and Afjeh, Abdollah A.: Non Conventional Fluid Film Bearings with Waved Surface. *Tribology*. INTECH, Vienna, Austria, 2011, in press.
- Feng, Guanping; and Xin, Nuan (1987): Automatic Control of the Vibration of the Flexible Rotor With Microcomputer. *J. Aero. Power*, vol. 2, pp. 199–203.
- Hemingway, E.W. (1967): A Performance Investigation Into the Elastically Stepped and Shrouded Thrust Bearing. *Proc. Instn. Mech. Engrs.*, vol. 182, pt. 1, no. 38, pp. 769–779. (References Kettleborough,

- C.F. (1957) Stepped Thrust Bearings, Proc. of Conf. On Lubrication and Wear, Proc. Inst. Mech. Engrs, Paper 37.)
- Hongo, Takeshi; Harada, Masami; and Miyaji, Ryutaro (1987): Static Characteristics of Externally Pressurized Gas Thrust Bearings With an Electrically Controlled Restrictor. *J. Japan Soc. Lubr. Engrs.*, vol. 32, no. 12, pp. 894–899 (Japanese).
- Lewis, G.K. (1984): The Stiffness and Static Stability of Compensated Hydrostatic Cylindrical-Pad Bearings. *Proc. Instn. Mech. Engrs.*, vol. 198, no. 16, pp. 285–292.
- Lund, J.W. (1968): Rotor-Bearing Dynamics Design Technology, Part 7: The Three-Lobe Bearing and Floating Ring Bearing. Mechanical Technology, Inc., Report MTI-67TR47 (AFAPL-TR-65-45, pt. 7, AD-829895), Feb. 1968.
- Martin, J.K. (1998): A Mathematical Model and Numerical Solution Technique for a Novel Adjustable Hydrodynamic Bearing. *Int. J. Numer. Meth. Fluids*, vol. 30, pp. 845–864.
- Mayer, J.E., Jr.; and Shaw, M.C. (1963): Characteristics of an Externally Pressurised Bearing Having Variable External Flow Restrictors. *J. Basic Eng.*, vol. 86, no. 2, pp. 291–296. (Discussion by Fox, G.R.; Mayer, J.E.; and Shaw, M.C. is on p. 296.)
- Morishita, Shin; and Ura, Tamaki (1993): ER Fluid Applications to Vibration Control Devices and an Adaptive Neural-Net Controller. *J. Intelligent Mat. Syst. Struct.*, vol. 4, no. 3, pp. 366–372.
- Palazzolo, A.B., et al., 1988: Piezoelectric Pushers for Active Vibration Control of Rotating Machinery. Rotordynamic Instability Problems in High-Performance Turbomachinery 1988, NASA CP-3026, pp. 87–110.
- Rowe, W.B.; Kilmister, G.T.F.; and Phil, M. (1974): A Theoretical and Experimental Investigation of a Self-Compensating Externally Pressurised Thrust Bearing. Paper D1, Proceedings of the 6th International Gas Bearing Symposium, N.G. Coles, ed., BHRA Fluid Engineering, Cranfield, U.K., pp. D1-1 to D-17.
- Rozeanu, L.; and Snarsky, L. 1978): Effect of Solid-Surface Lubricant Interaction on the Load Carrying Capacity of Sliding Bearings. *J. Lubr. Technol. Trans. ASME*, vol. 100, no. 2, pp. 167–175.
- Rylander, Grady H., et al. (1995): Actively Controlled Bearing Surface Profiles Theory and Experiments. Proceedings of the Energy-Sources Technology Conference and Exhibition, ASME, New York, NY, pp. 11–14.
- San Andres, L.A. (1992): Analysis of Hydrostatic Journal Bearings With End Seals. *J. Tribol.*, vol. 114, pp. 802–811.
- Sato, Y.; Maruta, K.; and Harada, M. (1988): Dynamic Characteristics of Hydrostatic Thrust Air Bearing With Actively Controlled Restrictor. *J. Tribol.*, vol. 110, no. 1, pp. 156–161.
- Schuller, Fredrick T. (1967): Lobing Technique for a Multilobed Bearing. NASA Case No. 11, 076, Disclosed Aug. 3, 1967. <http://ntrs.nasa.gov/>
- Schuller, Fredrick T. (1973): Design of Various Fixed-Geometry Water-Lubricated Hydrodynamic Journal Bearings for Maximum Stability. NASA SP-333.
- Stout, K.J.; Tawfik, M.; and Pink, E.G. (1978): Design of Externally-Pressurised Fluid-Film Bearings. *Eng.*, vol. 218, nos. 10–12, pp. 1046–1049, 1170–1173, and 1311–1314; and vol. 219, nos. 1–2, pp. 42–45 and 143–147. (References Girard, L.D. (1851): *Comptes Rendus*, Apr. 28–Oct. 6; Girard, L.D. (1863): *Application des Surfaces Glissantes*. Bachelier, Paris, p. 8; and Lord Rayleigh (1917): A Simple Problem of Forced Lubrication. *Engrg.*)
- Tieu, A.K. (1975): An Investigation of “Diaphragm” Type Thrust Bearings. Part I: Experiment. *J. Lubr. Technol. Trans.*, ASME Paper No. 75-Lub-K.
- Vekteris, V.J. (1993): Principles of Design and Classification of Adaptive Bearings. *Tribol. Trans.*, vol. 36, no. 2, pp. 225–230.
- Yoshida, Shinobu, et al. (1996): Non-Symmetrical Three-Lobe Bearing Spindle Technology: A Drive Technology to Increase Aerial Density. *IEEE Trans. Magnetics*, vol. 32, no. 3/2, May 1996, pp. 1721–1726.



- Yoshimoto, Shigeoka; Anno, Yoshiro; and Hirakawa, Yasushi (1994): Aerostatic Thrust Bearing With a Self-Controlled Restrictor Employing a Floating Disk. *JSME Int. J., Series C*, vol. 37, no. 2, pp. 369–375.
- Yoshimoto, Shigeoka; and Kamiyama, Shigeaki, (1995): Static Characteristics of an Aerostatic Journal Bearing With a Self-Controlled Restrictor Employing a Floating Brush. *Trans. Japan Soc. Mechanical Engineers, Part C*, vol. 61, no. 591 (Japanese), pp. 4443–4449.
- Yoshimoto, S.; and Kikuchi, K. (1999): Step Response Characteristics of Hydrostatic Journal Bearings With Self-Controlled Restrictors Employing a Floating Disk. *J. Tribology*, vol. 121, no. 2, ASME, pp. 315–320.
- Zaretsky, Erwin V. (1992): STLE Life Factors for Rolling Bearings. STLE SP–34, Park Ridge, Illinois.
- Zaretsky, Erwin V. (1997): Tribology for Aerospace Applications. STLE SP–37, Park Ridge, Illinois, pp. 494–495.

REPORT DOCUMENTATION PAGE			Form Approved OMB No. 0704-0188		
<p>The public reporting burden for this collection of information is estimated to average 1 hour per response, including the time for reviewing instructions, searching existing data sources, gathering and maintaining the data needed, and completing and reviewing the collection of information. Send comments regarding this burden estimate or any other aspect of this collection of information, including suggestions for reducing this burden, to Department of Defense, Washington Headquarters Services, Directorate for Information Operations and Reports (0704-0188), 1215 Jefferson Davis Highway, Suite 1204, Arlington, VA 22202-4302. Respondents should be aware that notwithstanding any other provision of law, no person shall be subject to any penalty for failing to comply with a collection of information if it does not display a currently valid OMB control number.</p> <p>PLEASE DO NOT RETURN YOUR FORM TO THE ABOVE ADDRESS.</p>					
<b>1. REPORT DATE (DD-MM-YYYY)</b> 01-01-2011		<b>2. REPORT TYPE</b> Technical Memorandum		<b>3. DATES COVERED (From - To)</b>	
<b>4. TITLE AND SUBTITLE</b> Active-Controlled Fluid Film Based on Wave-Bearing Technology			<b>5a. CONTRACT NUMBER</b>		
			<b>5b. GRANT NUMBER</b>		
			<b>5c. PROGRAM ELEMENT NUMBER</b>		
<b>6. AUTHOR(S)</b> Dimofte, Florin; Hendricks, Robert, C.			<b>5d. PROJECT NUMBER</b>		
			<b>5e. TASK NUMBER</b> YOM-5199		
			<b>5f. WORK UNIT NUMBER</b> WU-712-30-13-00		
<b>7. PERFORMING ORGANIZATION NAME(S) AND ADDRESS(ES)</b> National Aeronautics and Space Administration John H. Glenn Research Center at Lewis Field Cleveland, Ohio 44135-3191			<b>8. PERFORMING ORGANIZATION REPORT NUMBER</b> E-12841		
<b>9. SPONSORING/MONITORING AGENCY NAME(S) AND ADDRESS(ES)</b> National Aeronautics and Space Administration Washington, DC 20546-0001			<b>10. SPONSORING/MONITOR'S ACRONYM(S)</b> NASA		
			<b>11. SPONSORING/MONITORING REPORT NUMBER</b> NASA/TM-2011-210987		
<b>12. DISTRIBUTION/AVAILABILITY STATEMENT</b> Unclassified-Unlimited Subject Categories: 07 and 37 Available electronically at <a href="http://www.sti.nasa.gov">http://www.sti.nasa.gov</a> This publication is available from the NASA Center for AeroSpace Information, 443-757-5802					
<b>13. SUPPLEMENTARY NOTES</b>					
<b>14. ABSTRACT</b> It has been known since 1967 that the steady-state and dynamic performance, including the stability of a wave bearing, are highly dependent on the wave amplitude. A wave-bearing profile can be readily obtained by elastically distorting the stationary bearing sleeve surface. The force that distorts the elastic sleeve surface could be an applied force or pressure. The magnitude and response of the distorting force would be defined by the relation between the bearing surface stiffness and the bearing pressure, or load, in a feedback loop controller. Using such devices as piezoelectric or other electromechanical elements, one could step control or fully control the bearing. The selection between these systems depends on the manner in which the distortion forces are applied, the running speed, and the reaction time of the feedback loop. Using these techniques, both liquid- (oil-) or gas- (air-) lubricated wave bearings could be controlled. This report gives some examples of the dependency of the bearing's performance on the wave amplitude. The analysis also was proven experimentally.					
<b>15. SUBJECT TERMS</b> Wave bearing; Active control; Fluid film; Gas bearing; Rotordynamics					
<b>16. SECURITY CLASSIFICATION OF:</b>			<b>17. LIMITATION OF ABSTRACT</b>  UU	<b>18. NUMBER OF PAGES</b> 19	<b>19a. NAME OF RESPONSIBLE PERSON</b> STI Help Desk (email:help@sti.nasa.gov)
<b>a. REPORT</b> U	<b>b. ABSTRACT</b> U	<b>c. THIS PAGE</b> U			<b>19b. TELEPHONE NUMBER (include area code)</b> 443-757-5802



